Physica A 602 (2022) 127650

Contents lists available at ScienceDirect

Physica A

journal homepage: www.elsevier.com/locate/physa

A theory of coalescence of signaling receptor clusters in immune cells

V.M. Kenkre [a,1], K. Spendier [b,*,1]

[a] Department of Physics and Astronomy, University of New Mexico, 210 Yale Blvd NE, Albuquerque, 87131, NM, USA
[b] Department of Physics and Energy Science and UCCS Center for the Biofrontiers Institute, University of Colorado Colorado Springs, 1420 Austin Bluffs Pkwy, Colorado Springs, 80918, CO, USA

ARTICLE INFO

Article history:
Received 19 June 2021
Received in revised form 8 April 2022
Available online 2 June 2022

Keywords:
Random walk aggregation
Coalescence via diffusion

ABSTRACT

A theory of coalescence of signal receptor clusters in mast cells is developed in close connection with experiments. It is based on general considerations involving a feedback procedure and a time-dependent capture as part of a reaction–diffusion process. Characteristic features of observations that need to be explained are indicated and it is shown why calculations available in the literature are not satisfactory. While the latter involves *static* centers at which the reaction part of the phenomenon occurs, by its very nature, coalescence involves dynamically evolving centers. This is so because the process continuously modifies the size of the cluster aggregate which then proceeds to capture more material. We develop a procedure that consists of first solving a static reaction–diffusion problem and then imbuing the center with changing size. The consequence is a dependence of the size of the signal receptor cluster aggregate on time. A preliminary comparison with experiment is shown to reveal a sharp difference between theory and data. The observation indicates that the reaction occurs slowly at first and then picks up rapidly as time proceeds. Parameter modification to fit the observations cannot solve the problem. We use this observation to build into the theory an accumulation rate that is itself dependent on time. A memory representation and its physical basis are explained. The consequence is a theory that can be fit to observations successfully.

1. Introduction and background

Cells in a multicellular organism must be ready to respond to a variety of extracellular signals [1]. Incorrect interpretation or translation of such signals can result in diseases such as cancer. Extracellular signals include ligands on the surface of cells, parasites, or allergens that can bind to cell surface receptors in the target cell membrane. Such transmembrane signaling through receptor–ligand interaction plays important roles in immune responses. Our primary interest is immune signaling by mast cells. Mast cells store granules with chemical mediators of inflammation. These mediators are released when high-affinity Fc receptors (FcϵRI) specific for immunoglobulin E (IgE) are brought into proximity, i.e. aggregated.

In model systems, receptor aggregation is usually accomplished by cross-linking IgE-loaded receptors with multivalent ligands [2] or by monovalent ligands bound to a fluid lipid bilayer [3–7]. In the latter model system as shown in Fig. 1, the receptors are first aggregated in microclusters and then move by apparently performing diffusion or random walk motion [5] to eventually coalesce to form a big central receptor patch, called the mast cell synapse [4]. The development of

* Corresponding author.
E-mail address: kspendie@uccs.edu (K. Spendier).

[1] V.M. Kenkre and K. Spendier have contributed equally to all aspects of writing this paper.

https://doi.org/10.1016/j.physa.2022.127650
0378-4371/

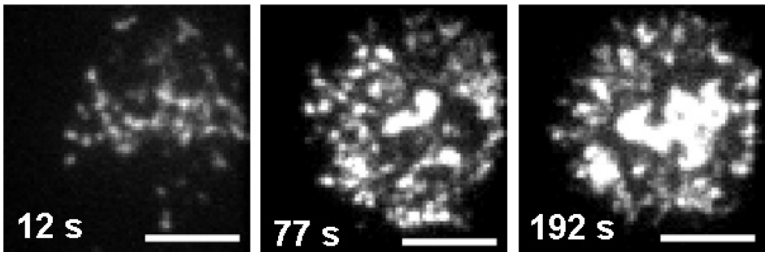

Fig. 1. Time-laps of receptor cluster coalescence. Total internal reflection fluorescence microscope images of mast cell loaded with fluorescent IgE-receptor complexes pipette-pressed onto a fluid lipid POPC bilayer with 25 mol% DNP lipid after 12 s, 77 s, and 192 s of initial contact. Large-scale reorganization of fluorescent receptors into a synaptic-like structure occurs within 3 min at 37 °C. Scale bar represents 5 μm.

such spatial patterns of receptors and the consequence for mast cell signaling is likely to be important for the interactions of mast cells with various parasites [8]. To understand this most basic mast cell role, the underlying kinetics of synapse formation in mast cells need to be understood. In this paper, we construct a simplified theory for receptor microcluster coalescence based on our experimental observations.

Similar large-scale receptor clustering due to monovalent ligands in fluid membranes has been observed in other immune cells, namely *T* cells and B cells [9,10]. In these immune systems, the large central patch is called an immunological synapse. The immunological synapse is thought to play a critical role in immune cell signaling between contacting cells [9]. Therefore, the kinetics of synapse formation in *T* cells [11–13] and B cells [14–16] have been modeled extensively. However, we have shown that important model parameters in *T* cell and B cell systems such as a second receptor–ligand pair and centripetal cluster motion are not essential in the kinetics of mast cell synapse formation. Therefore, existing theories of coalescence of signaling receptor clusters in immune cells cannot be applied directly to the mast cell system.

Further motivation to develop a new coalescence theory is given by shortcomings in existing theories, whose aim is to describe particle aggregation or absorption. The simple problem of a stationary absorber in three dimensions was first solved by Smoluchowski [17]. In this problem, a spherical stationary absorber is embedded into a distribution of Brownian particles. He derived the reaction rate of Brownian particles with the sphere as the product of the surface area of the absorber times the particle flux. That analysis assumes perfect absorption which means that it does not describe particles that react at a finite rate. In using that analysis, modern theories of aggregation have typically simply multiplied the Smoluchowski reaction rate by a probability of merging [18,19], resulting in a transition rate described by a *product* of the probabilities. This, however, is seldom legitimate. This aspect of reaction–diffusion, i.e., imperfect absorption in the reaction process presents a fundamental problem investigated thoroughly in a series of papers [20–27] in the context of exciton transport and sensitized luminescence.[2]

For instance, Ref. [22] shows that the exciton trapping time can be best described as the sum of the time it takes to move to the trap and the time it takes to get captured while at the site. This is not an assumption but the result of the mathematical development. This led us first to reexamine the analysis of the signal receptor cluster absorption problem. We found out that the standard use of the Smoluchowski reaction rate analysis suffered from another shortcoming in that the effect produced on the diffusion field by the moving boundary of the stationary absorber seemed not to be taken properly into account. A small collection of moving-boundary problems, which can be solved exactly, can be found in Refs. [28–30]. It is noteworthy that it has been long recognized that the motion of the moving boundary must perturb the diffusion field and hence several attempts have been made to model this effect [29,31,32]. We decided, therefore, to construct our own analysis considering these various items and to be guided closely by our experimental coalescence observations.

2. Reaction diffusion formalism and static expression

Focusing on our experimental observations outlined in Section 3, we address the following simplified problem. We start with a certain amount of material that is divided into two parts. The first part is made into a disk of uniform density and radius $R(0)$ placed with its center at the origin. This disk represents the nucleation site of the central receptor patch observed in our experiments. The initial disk radius is given by experimental observations. The rest of the material of which the amount is $Q(0)$ is taken to consist of random walking point particles throughout the two-dimensional space outside the disk with a given known distribution.

As time proceeds, the point particles move in an appropriate type of motion, e.g. that we take to be purely diffusive for simplicity until they touch the edge of the disk. With non-infinite probability (finite capture rate) the particles are

[2] The interested reader might want to examine an entire chapter (Chapter 11) of a recently published book, most of that chapter having been constructed to discuss this significant issue in the context of molecular crystals: Kenkre V. M. (2021) Memory Functions, Projection Operators, and the Defect Technique: Some Tools of the Trade for the Condensed Matter Physicist. Springer Nature.

absorbed into the disk. The process of absorption makes the disk attain a larger radius. In other words, we make the simplifying assumption that the *shape* of the disk does not change. What changes is the radius $R(t)$ of the disk. And this occurs not necessarily instantaneously but could involve a rearrangement process that takes some finite time. We start assuming it to be instantaneous, find the result incompatible with what is observed, and modify the theory to accommodate the observation. This is an important ingredient, which makes our coalescence theory differ from processes such as diffusion-limited aggregation [33,34], where finger-like structures develop. The purpose of the rest of the study is then to calculate the evolution of $R(t)$. For simplicity at this stage of the calculation, the point particles do not absorb one another, although in the experiments described in Section 3 the contrary is certainly observed. This is a detail that will be incorporated into the theory in the future.

Our simplified study may be formulated as a trapping problem with a trap whose location (boundary) changes dynamically. The analysis proceeds by solving the appropriate trapping problem and obtaining an expression for $Q(t)$ (total survival probability at time t) the amount of the sprinkled material not yet absorbed into the central disk. We thus begin our analysis with the standard defect technique [20] but find it natural to modify it during the process of application to the observations.

The natural connection between $Q(t)$ and $R(t)$ can be made through the area of the growing disk, more specifically the area A of a growing ring, with inner radius $R(0)$ and outer radius $R(t)$, is given by $\pi\left(R(t)^2 - R(0)^2\right)$. This area must be proportional to $Q(0) - Q(t)$, where the initial amount of material, $Q(0)$, equals one. After applying the initial condition that the area of the ring must be zero at time zero and it must be $\pi\left(R(\infty)^2 - R(0)^2\right)$ at infinite time, where the final radius of the circular trap is $R(\infty)$, we arrive at

$$\frac{R^2(t) - R^2(0)}{R^2(\infty) - R^2(0)} = \frac{Q(0) - Q(t)}{Q(0) - Q(\infty)}. \tag{1}$$

The exponent of $R(t)$ and $R(0)$ will change according to the dimensionality of the system. Here we take it to be 2. Eq. (1) starts from zero and rises to one and can be readily compared to experiment once $Q(t)$ is known. The initial radius $R(0)$, the final radius $R(\infty)$, and $Q(\infty)$ are readily available from experiment. We normalize the initial amount of material to $Q(0)$=1. For two-dimensional radial symmetric trapping problems, exact expressions for $Q(t)$ can be obtained only in the Laplace domain. Application of numerical inversion schemes can be applied to calculate the exact functional form for $Q(t)$ in time domain [35,36].

2.1. Reaction diffusion formalism

To incorporate the items of analysis that we have discussed above we formulate our reaction–diffusion formalism on the basis of a 2-dimensional diffusion equation [27] describing the movement of the material with diffusion constant D from outside a central disk of radius R to its circumference (border) and be captured by the disk border at a certain rate C_2. Such an equation would have the form in Cartesian coordinates, obeyed by the probability density $P(x, y, t)$ of the material at the point (x, y) at time t,

$$\begin{aligned}\frac{\partial P(x,y,t)}{\partial t} &= D\left(\frac{\partial^2 P(x,y,t)}{\partial x^2} + \frac{\partial^2 P(x,y,t)}{\partial y^2}\right) \\ &\quad - \sum_r{}' \delta(x - x_r)\delta(y - y_r)C_2 P(x,y,t),\end{aligned} \tag{2}$$

the r-summation over the points with coordinates (x_r, y_r) being on the circumference of the representative disk. The prime on the summation symbol describes the fact that those points constitute the defect region where material is captured. Here C_2 is the two dimensional capture rate with unit of length squared divided by time. The actual movement is, needless to state, in 3-dimensional space. However, numerous studies by us and others have indicated that provided the extent of the motion is bounded in the additional (third dimension) an accurate representation is provided when the extent is small in the third dimension, by a 2-dimensional calculation. The latter is more didactic when used in the analysis because it avails of the small spatial extent in the additional dimension.[3] Due to cylindrical symmetry, (which becomes polar symmetry in the 2-dimensional representation here of the 3-dimensional cylindrical cell), trapping is occurring throughout the border of this disk which results in an integration over the polar angle θ. It is useful to rewrite this equation in polar coordinates

$$\begin{aligned}\frac{\partial P(r,\theta,t)}{\partial t} &= D\frac{\partial^2 P(r,\theta,t)}{\partial r^2} + D\left(\frac{1}{r}\frac{\partial P(r,\theta,t)}{\partial r} + \frac{1}{r^2}\frac{\partial^2 P(r,\theta,t)}{\partial \theta^2}\right) \\ &\quad - \frac{2\pi}{r}\delta(r - R)C_2 P(r,\theta,t).\end{aligned} \tag{3}$$

[3] Such supporting studies are not only numerical and can be produced at a moment's notice but also analytical as suggested by the use made by Fort et al. [37] in their analysis of triplet motion in molecular crystals on the basis of the approximate representation of Bessel function propagators. This is the natural reason we have used a 2-dimensional analysis based on disks rather than a 3-dimensional counterpart in cylinders.

Next we integrate the probability distribution $P(r,\theta,t)$ given in Eq. (3) over all space outside the disk border, giving the material

$Q(t) = \iint drd\theta rP(r,\theta,t)$ that has still survived without being absorbed, or for the rate of disappearance, $dQ(t)/dt$,

$$\frac{dQ}{dt} = \iint drd\theta r \frac{\partial P(r,\theta,t)}{\partial t}. \tag{4}$$

An equation such as Eq. (2) written as it was originally [23,24,27,38] formulated leads to the survival probability Q in the Laplace domain expressed as:

$$\widetilde{Q}(\epsilon) = \frac{1}{\epsilon}\left[1 - \frac{\sum_r' \widetilde{\eta}(x_r,\epsilon)}{1/C_d + \sum_r' \widetilde{\Pi}(x_r,x_r,\epsilon)}\right], \tag{5}$$

and ϵ is the Laplace transform variable. Here $\widetilde{\Pi}(x_r,x_r,\epsilon)$ is the self-propagator, $\widetilde{\eta}(x_r,\epsilon)$ is the homogeneous solution at the trap site in the absence of the trap, $\sum_r'$ represents the sum over all trap sites which becomes an integral over the boarder of the disk here, the x_r denote vectors in the appropriate number of dimensions, and C_d is the d-dimensional capture parameter. The units of the capture parameter depend on the difference between the number of dimensions of the overall region in which motion occurs and the number of dimensions in which capture occurs. As derived in Ref. [39] and explained in detail in Section 6.5 of a recent book [40], the capture parameter has units of reciprocal time if these numbers are identical. But in our present case where the motion occurs in 2-dimensions but capture is 1-dimension, the parameter C_d has units of area divided by time. In Eq. (5) we use tilde$\widetilde{}$to denote a Laplace transform. We refer the reader to explicit derivations of Eq. (5) available at the places indicated and mention here only that physically it can be said to arise from the renormalized statement of the rate of the survival probability being proportional to the probability in the capture region.

Using this prescription in the continuum in which the point propagator becomes a radial propagator due to cylindrical symmetry, one can calculate $Q(t)$ for an initial circular symmetric distribution of diffusing non-interacting point particles initially at R_0. The circular trap is centered at the origin and has a radius R. The radial propagator can be calculated from the probability density for the particle to occupy the circumference of radius R given that it initially occupied that of radius r,

$$P(R,r,t) = \frac{1}{4\pi Dt} e^{-\frac{r^2+R^2}{4Dt}} I_0\left(\frac{rR}{2Dt}\right). \tag{6}$$

as was done in [27]. Here I_0 is the zero-order modified Bessel function. In the probability density function above, we put $r = R$ to calculate the self-propagator

$$\Pi(R,R,t) = \frac{1}{4\pi Dt} e^{-\frac{R^2}{2Dt}} I_0\left(\frac{R^2}{2Dt}\right) \tag{7}$$

and $r = R_0$ to get homogeneous solution at the trap ring

$$\eta(R,R_0,t) = \frac{1}{4\pi Dt} e^{-\frac{R^2+R_0^2}{4Dt}} I_0\left(\frac{RR_0}{2Dt}\right). \tag{8}$$

If we Laplace transform both expressions and substitute them in Eq. (5), we obtain

$$\widetilde{Q}(\epsilon) = \frac{1}{\epsilon}\left[1 - \frac{\frac{1}{2\pi D} K_0\left(\sqrt{\frac{\epsilon}{\gamma_0}}\right) I_0\left(\sqrt{\frac{\epsilon}{\epsilon_0}}\right)}{\frac{1}{C_2} + \frac{1}{2\pi D} K_0\left(\sqrt{\frac{\epsilon}{\epsilon_0}}\right) I_0\left(\sqrt{\frac{\epsilon}{\epsilon_0}}\right)}\right], \tag{9}$$

where $\epsilon_0 = D/R^2$ and $\gamma_0 = D/(R_0^2)$. Here $K_n(z)$ is the nth order modified Bessel function of the second kind. Eq. (9) describes a permeable trapping boundary. However, experimental observations indicate that the central trap grows only after a successful receptor patch melding event. Therefore, an expression for impermeable membranes and finite reaction rate must be used. Fortunately, such expressions are available readily from previous investigations of the equivalence between the stationary trapping theory and the theory of conduction in heat and solids because of translational invariance of the propagator in the absence of a capture process [27,41]. For this purpose, we use Carslaw and Jaeger [42] with the substitution of the reaction rate with $C_2/[2\pi DR(0)]$ as outlined in detail in our previous work [27] to obtain an expression for an initial distribution of particles along a ring of radius r_0

$$\widetilde{Q}(\epsilon, r_0) = \frac{1}{\epsilon} \times \left\{1 - \frac{K_0\left[r_0\sqrt{\frac{\epsilon}{D}}\right]}{\frac{2\pi DR(0)}{C_2}\sqrt{\frac{\epsilon}{D}} K_1\left[\sqrt{\frac{R(0)^2\epsilon}{D}}\right] + K_0\left[\sqrt{\frac{R(0)^2\epsilon}{D}}\right]}\right\}. \tag{10}$$

Table 1
Essential model parameters pertaining to experimental data available in Ref. [46]. Values represent the mean ± corresponding standard deviation obtained from five different data sets.

Parameter	Value
Cluster diffusivity, D	0.011 ± 0.004 $\mu m^2/s$
Initial cluster size, $R(0)$	1.1 ± 0.2 μm
Final patch size, $R(\infty)$	3.2 ± 0.4 μm
Cell-substrate contact radius, r_0'	5.75 ± 0.66 μm
Amount of material not absorbed, $Q(\infty)$	0.26 ± 0.11

In our experiments [5], we observed that the number of clusters found at a radial distance r from the center of the cell-substrate contact area is proportional to r. Since the radius of the contact area, r_0' can be estimated from experiments, the survival probability can be written as a superposition by integrating Q over the normalized initial point-particle distribution

$$\widetilde{Q}(\epsilon) = \frac{2}{r_0'^2 - R(0)^2} \int_{R(0)}^{r_0'} \widetilde{Q}(\epsilon;\ r_0)\, r_0\, dr_0. \tag{11}$$

Note that the lower limit of the integration is $R(0)$. After integrating $\widetilde{Q}(\epsilon, r_0)$ given in Eq. (10) over the initial particle distribution, using

$$\int_{R(0)}^{r_0'} r_0 K_0\left[r_0\sqrt{\frac{\epsilon}{D}}\right] dr_0 = \sqrt{\frac{R(0)^2 D}{\epsilon}} K_1\left[\sqrt{\frac{R(0)^2\epsilon}{D}}\right] - \sqrt{\frac{r_0'^2 D}{\epsilon}} K_1\left[\sqrt{\frac{r_0'^2\epsilon}{D}}\right] \tag{12}$$

one obtains

$$\widetilde{Q}(\epsilon) = \frac{1}{\epsilon} - \frac{2}{\epsilon\left[1 - \frac{R(0)^2}{r_0'^2}\right]} \times \left\{ \frac{\frac{R(0)}{r_0'} K_1\left[\frac{R(0)}{r_0'}\sqrt{\tau\epsilon}\right] - K_1\left[\sqrt{\tau\epsilon}\right]}{\xi\tau\epsilon K_1\left[\frac{R(0)}{r_0'}\sqrt{\tau\epsilon}\right] + \sqrt{\tau\epsilon} K_0\left[\frac{R(0)}{r_0'}\sqrt{\tau\epsilon}\right]} \right\}. \tag{13}$$

Here, the dimensionless parameters are defined as $\tau = (r_0')^2/D$ and $\xi = 2\pi D R(0)/[C_2\ r_0']$. Eq. (13) is one of the two equations connecting Q and R. This equation only works when the radius of the trapping disk is unchanged during the capture process. However, the radius of the disk is changing and hence Eq. (13), after numerical inverse-Laplace transformation, is substituted into Eq. (1) to obtain an expression that describes the growing radius $R(t)$ of the central disk that is observed in experiment. We perform a direct comparison of these two simultaneous equations to experiments in the next section.

3. First comparison to observations and quantitative failure

To investigate receptor cluster coalescence in mast cells, the rat basophilic leukemia 2H3 (RBL) cell line was used as a model [4–7,43–45]. Experimental data that is available for use in Ref. [46], was obtained from total internal reflection fluorescence (TIRF) images of fluorescently labeled IgE-FcϵRI complexes pipette-pressed onto a fluid ligand presenting bilayer. When a RBL cell loaded with fluorescent IgE contacted a monovalent ligand bearing fluid lipid bilayer, receptor microclusters instantaneously appeared and brightened within seconds due to receptor trapping at close points of contact between the cell and the substrate [5]. After receptor microclusters formed they moved with both a diffusive and directed motion component and coalesced to form a big central patch [4–7]. This largest receptor patch predominantly formed in the center of the cell-substrate contact zone [8] of radius r_0' which was estimated from data available in Ref. [46]. Using this data, we also estimated an average receptor cluster diffusion coefficient D using temporal image correlation analysis [47]. The initial radius of the central receptor patch $R(0)$, the final central patch radius $R(\infty)$, and the average amount of material not yet absorbed $Q(\infty)$, were obtained by an image thresholding technique. Briefly, we used ImageJ's [48] particle analyze tool to calculate receptor cluster and receptor patch radii at each time point for five different cells. Corresponding parameter values are listed in Table 1. Additionally, the previous analysis showed further that clusters are initially randomly distributed [5] and that the initial average distance between two clusters was 350 nm. Cluster motion, of cluster diameters from 0.4 to 1.2 μm, did not depend on size [8]. Qualitatively, not every cluster–cluster contact resulted in coalescence, rather cluster coalescence occurred at a finite rate. Moreover, our experimental observations suggested that at early times of cell-substrate contact (<1 min), receptor clusters did not coalesce on contact. Only at late times was the merging process more frequent. Accordingly, the receptor cluster size-time curve is characteristically sigmoidal (see Fig. 2).

Fig. 2 fits the experimental data (black error bars) to Eq. (1) after numerical inverse-Laplace transformation of Eq. (13), using the mean value of experimental parameters given in Table 1 and extracting the mean of the maximum receptor

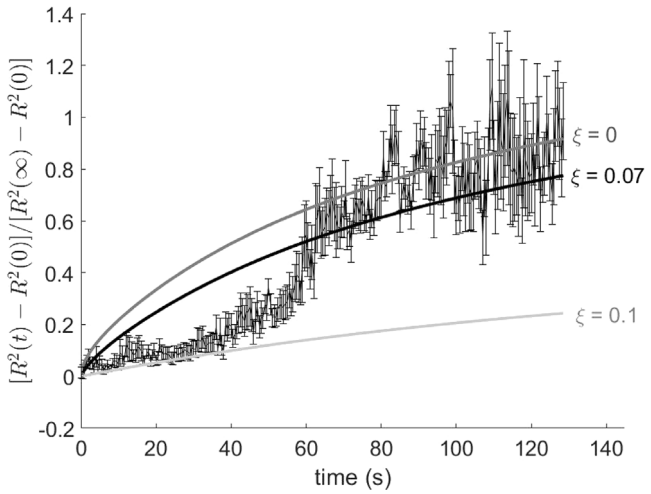

Fig. 2. Failure of the simple theory. Comparison of data to a coalescence theory for finite coalescence probability given in Eq. (13) with inverse-Laplace transforming Eq. (13) for $\xi = 0$ (instantaneous coalescence for $C_2 \to \infty$), best fit $\xi = 0.007$, and $\xi = 0.1$. The bars represent the error obtained from the propagation of errors using the standard error of the mean obtained from five individual cell data sets.

cluster or receptor patch radius at each time point, $R(t)$. The only fitting parameter was finite capture rate C_2. The best fit is shown by the solid black line with dimensionless capture parameter $\xi = 2\pi DR(0)/[C_2\, r_0'] = 0.007$. The best fit was performed by minimizing chi-squared

$$\chi^2 = \sum_{i=1}^{N} \left(\frac{f(x_i) - \mu_i}{\sigma_i} \right)^2 . \tag{14}$$

Here $N = 251$ is the number of data points in the time series, μ_i is the observed mean of the data with a standard deviation σ_i, and $f(x_i)$ is the predicted mean obtained from Eq. (1). For comparison, gray lines show instantaneous coalescence ($\xi = 0$) as well as higher values of the capture parameter, $\xi = 0.1$.

From this direct comparison of theory and experiment, we conclude the following. At early time < 60 s, experimentally observed receptor cluster coalescence in mast cells, when presented to a fluid ligand-bearing membrane, seems to be delayed. This observation suggests that our coalescence theory for a constant capture rate does not explain our experimental data at early time. The observation motivates us to develop a theory that considers a time dependence of the reaction rate as outlined in the next section. Such a time-dependent change in reaction rate might be due to a biological or kinetic response mechanism, which is coupled to the observed delay in cluster coalescence, leading to a coalescence process that is non-local in time.

4. Time dependence of reaction rate and a memory representation

The rearrangement of material absorbed into the central disk is not instantaneous. If it were, we could consider the solution of the two simultaneous equations relating the disk radius, $R(t)$, and the quantity of material not yet absorbed, $Q(t)$. To remain compatible with our simplified assumption that we consider the disk always circular, we must allow for the finite time taken by rearrangement. This means that the capture process must be considered time-dependent, i.e., C_2 must be considered time-dependent. However, analytical procedures for treating an equation such as Eq. (3) but with a time-dependent C_2, are not available, the defect technique's primary tool being Laplace transformation. It turns out, however, that a capture process represented through a *memory* function, which means through a convolution, is perfectly natural to the formal procedure involved in the defect technique. We will discuss the relationship of a time-dependent capture to a memory capture function in Section 6 below. For now, we generalize Eq. (3) for this purpose specifically into the form

$$\begin{aligned} \frac{\partial P(r,\theta,t)}{\partial t} &= D\frac{\partial^2 P(r,\theta,t)}{\partial r^2} + D\left(\frac{1}{r}\frac{\partial P(r,\theta,t)}{\partial r} + \frac{1}{r^2}\frac{\partial^2 P(r,\theta,t)}{\partial \theta^2} \right) \\ &\quad - \frac{2\pi}{r}\delta(r-R)\left[\int_0^t ds \mathcal{C}(t-s) P(r,\theta,s) \right], \end{aligned} \tag{15}$$

where $\mathcal{C}$ is the capture memory. The evolution of $P(r,\theta,t)$ would then depend not only on the current time t but prior times s as well. The only modification of a result such as Eq. (15) for Q in Laplace domain, with no change except the

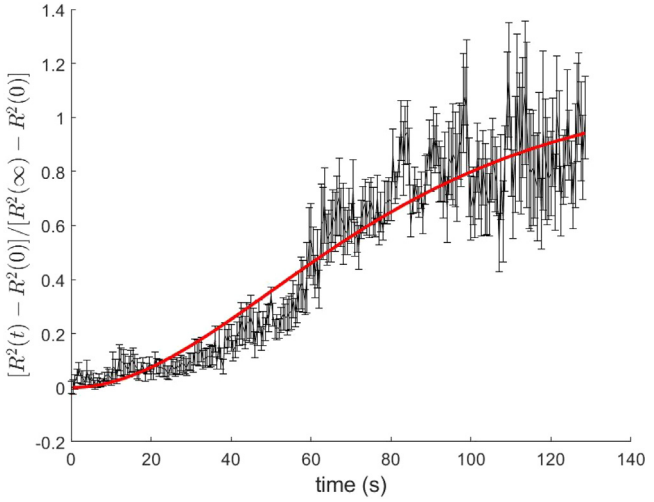

Fig. 3. The success of the theory when a memory-dependent capture is incorporated and extraction of system parameters C_2 and α. Best fit procedure with Eq. (1) results in $\alpha = 33 \times 10^{-12}/s$ and $\alpha C_2 = 0.12$ m^2/s^2. The bars represent the error obtained from the propagation of errors using the standard error of the mean obtained from five individual cell data sets.

replacement of the constant C_2 by the Laplace transform of the capture memory $\widetilde{\mathcal{C}}(\epsilon)$, is

$$\widetilde{Q}(\epsilon) = \frac{1}{\epsilon}\left[1 - \frac{\sum_r' \widetilde{\eta}(x_r, \epsilon)}{1/\widetilde{\mathcal{C}}(\epsilon) + \sum_r' \widetilde{\Pi}(x_r, x_r, \epsilon)}\right]. \tag{16}$$

We now choose the capture memory in the time domain as $\mathcal{C}(t) = C_2\alpha e^{-\alpha t}$ for the twin purpose of simplicity and for convenience to return to a memory-less capture situation by taking the limit $\alpha \to \infty$ and thereby making the memory $C_2\delta(t)$. The result is

$$\widetilde{Q}(\epsilon) = \frac{1}{\epsilon} - \frac{2}{\epsilon\left[1 - \frac{R(0)^2}{r_0'^2}\right]} \times \left\{\frac{\frac{R(0)}{r_0'}K_1\left[\frac{R(0)}{r_0'}\sqrt{\tau\epsilon}\right] - K_1\left[\sqrt{\tau\epsilon}\right]}{\frac{2\pi DR(0)(\epsilon+\alpha)}{C_2\alpha\, r_0'}\tau\epsilon K_1\left[\frac{R(0)}{r_0'}\sqrt{\tau\epsilon}\right] + \sqrt{\tau\epsilon}K_0\left[\frac{R(0)}{r_0'}\sqrt{\tau\epsilon}\right]}\right\}, \tag{17}$$

which is the first of the two simultaneous equations relating the quantity of material not yet absorbed, $Q(t)$, and the disk radius, $R(t)$, given in Eq. (1) for the case of non-instantaneous rearrangement of material being absorbed into the central disk.

5. Success in agreement with observation

Qualitative experimental evidence as presented in Section 3 suggests that the observed delay is connected to a time-dependent coalescence probability; at early times of cell-substrate contact, cluster–cluster contact does not lead to coalescence, whereas at later times almost every contact of two clusters leads to coalescence. We now employ a generalization of our coalescence theory with a trapping process characterized by a memory kernel as outlined above, in Section 4. A comparison of this model given in Eq. (1) with inverse-Laplace transforming Eq. (17) is depicted in Fig. 3.

The theoretical curve (depicted in red) results in a much improved fit of our generalized theory with exponential memory $\mathcal{C}(t) = C_2\alpha e^{-\alpha t}$ and best fit $\alpha = 33 \times 10^{-12}$/s and $\alpha C_2 = 0.12$ m^2/s^2. Other parameters are known from the experiment and given in Table 1. The comparison clearly shows that the biological receptor cluster coalescence delay can be qualitatively explained by a time-dependent capture memory with a characteristic time of the order of several tens of picoseconds. It is comforting to realize that there are specific biological processes that occur at such short time scales, exemplified by enzymatic activity.[4]

[4] For example, adenylate kinase is an enzyme that controls the energy balance in cells by catalyzing adenosine triphosphate (ATP) and adenosine monophosphate (AMP) into two adenosine diphosphate (ADP) molecules [49]. For this kinase, fluctuations on the picosecond time scale have been experimentally linked with protein dynamics on the micro- to millisecond range [50]. Initial IgE-FcϵRI receptor cluster formation in RBL cells, when presented to a fluid ligand-bearing membrane, also occurs in the millisecond range [5].

6. Discussion

Coalescence of signal receptor clusters in mast cells is an important phenomenon, experiments carried out by one of the authors (K.S.) have indicated characteristic features that must be explained, and existing theories are wanting in several respects. We have undertaken the construction of our own theory for the process which we have explained in the preceding sections. It is based on interesting new concepts, fails in its simplest form but succeeds in its more mature form. The preliminary failure and the eventual success are both instructive. Comparison of theory to observations allows us to extract system parameter values that are reasonable. We discuss now the manner in which we have arrived at the theory in this final Section.

Coalescence involves centers that evolve in time as they move and come together. The processes of their motion and their combination are therefore important to understand, both individually and as they interact with each other. Previous attempts to address the phenomenon by employing Smoluchowski arguments and using the subterfuge of multiplying the reaction rate by a probability of merging [18,19] are not appropriate as shown by several examinations carried out in reaction–diffusion scenarios in other systems [20–27]. There are several features of the coalescence phenomenon that require deeper consideration including the fact that it involves moving boundaries where the reaction–diffusion process occurs.

Our method starts by focusing on point particles constituting the material moving in a simplified 2-dimensional space outside a central region. Their meeting the borders of the central region (taken as a circular disk that increases in radius as material attaches to it) causes the coalescence. Taking the moving material as made of particles of no size and neglecting their coalescence with one another leading to the formation of disks of finite size in addition to the central disk are assumptions justified by simplicity in the calculation. It is hoped that further steps in the theory will relax these restrictions. The motion turns out to be clearly diffusive and therefore a random walk is envisaged. A finite rate of blending with the central disk is assumed. The defect theory developed for instance in [38] is applied in a circular geometry, as in [27], in a form that is recognizable also from the work of Carslaw and Jaeger [42]. The starting equation is Eq. (3).

The method then proceeds with the help of two equations that relate the time dependence of the central expanding disk radius $R(t)$ to the material amount $Q(t)$, Eq. (1), and Eq. (5) which for the circular geometry takes the form of Eq. (13). The latter has in its information about the initial radius of the disk and information about the geometry through Laplace transforms of K-Bessel functions. The basic idea is to use the defect technique of Montroll [51] to calculate the accumulation of material into the disk, the latter process to augment the radius and thereby move the boundary and thus, in a feedback manner, to build up the size of the central disk.

The favorable features of this theory are the correct treatment of the accumulation process by avoiding the multiplication of probabilities that has been part of earlier analysis and using the feedback process so that the moving boundary effect is incorporated. Perhaps surprisingly, the theory fails spectacularly when compared with observations. This is seen in Fig. 2.

It is evident that it is not a question of merely choosing alternate parameters for the system. The failure points clearly to the fact that the experiment displays multiple time constants in the evolution of the radius which is sigmoidal in nature. The recognition of the need for two time constants leads to modifying the theory first to include a time-dependent capture rate $C_2(t)$ and then, for computational ease to include a capture memory $\mathcal{C}(t)$.

What leads to a time-dependent capture rate or a capture memory? And what is the meaning of the connection between these two ways of including the process in the analysis? These are two questions that need to be answered. We treat them in reverse order.

6.1. Memory representation of a time-dependent capture process

There are many instances in statistical mechanics where we come across the need to approximate a convolution type of term

$$\int_0^t ds\, a(t-s)b(s) = \int_0^t ds\, a(s)b(t-s)$$

where one of the functions a, b is much more rapidly varying in time (t and s stand for time) than the other. Let us take the slowly changing function to be b. The *half-Markoffian* approximation [20,52–54] consists of taking this slow function out of the integral and performing the integral of the fast function, $\left(\int_0^t ds\, a(s)\right)$ as $A(t)$, such that we can write

$$\int_0^t ds\, a(t-s)b(s) \approx A(t)b(t). \tag{18}$$

Let us briefly examine the validity of such an approximation. Let us consider a term

$$I(t) = \int_0^t ds\, \beta e^{-\beta(t-s)} e^{-s^2}, \tag{19}$$

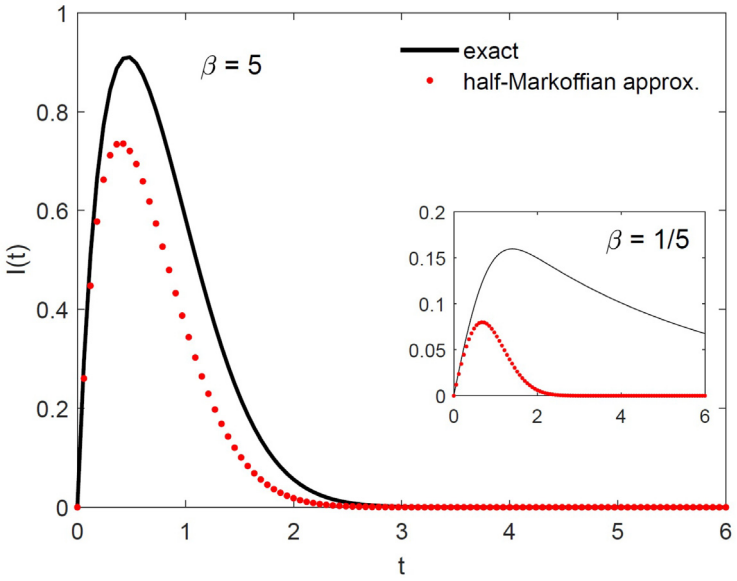

Fig. 4. Examination of the validity of the half-Markoffian approximation. The exact expression is $I(t)$ as in Eq. (20), see text (black solid line). The approximate expression (red dots), obtained by pulling the slow factor out of the integrand but maintaining the upper limit of integration as t, and doing the integral of the fast factor, is Eq. (21). The main figure shows the case of large $\beta = 5$ (time variations of the two factors of the integrand disparate). The approximation is reasonable both at short and long times. Insets show the cases $\beta = 1/5$ which means the variation is disparate but the fast one is taken out of the integration. This case shows the approximation to be bad. In our analysis we use the approximation in reverse: to replace a product of time functions by a convolution. See text.

which is at once evaluated exactly in terms of the error functions $\mathrm{erf}(y) = (2/\sqrt{\pi}) \int_0^y dz\, e^{-z^2}$ as

$$I(t) = \beta e^{\beta^2/4} (\sqrt{\pi}/2) e^{-\beta t} \left[\mathrm{erf}(t - \beta/2) - \mathrm{erf}(-\beta/2)\right]. \tag{20}$$

If we were to make the half-Markoffian approximation on $I(t)$, taking $\beta e^{-\beta t}$ as the rapidly varying function a, the result of the half-Markoffian approximation is to represent $I(t)$ as

$$I(t) = e^{-t^2} \left(1 - e^{-\beta t}\right). \tag{21}$$

Fig. 4 shows a comparison of the exact result Eq. (20) for $I(t)$ with the approximate representation Eq. (21) for two values of β: 5 in which case (shown in the main figure) the exponential is certainly rapidly varying relative to the Gaussian, and 1/5 (shown in the inset of the figure) in which it is not. We see that the latter case is hopeless as an approximation but the former case shows itself to be a fine approximation both qualitatively and quantitatively for small and large times in particular.[5]

That the failure of a description via a process of capture involving a single time constant viz., the reciprocal of the capture rate, is clear from Fig. 2. Armed with this assurance of the half-Markoffian approximation as a reasonable procedure, we incorporate it in our problem in reverse, i.e., approximate a product of two functions in time by a convolution.

6.2. Rearrangement process that leads to a time-dependent capture process

Comparison to experiment, as shown in Fig. 2, has made it essential that the theory we have constructed should incorporate time-dependence in the capture process (equivalently, the memory phenomenon). The idea comes from the rearrangement process that makes the radius $R(t)$ of the growing disk evolve into a new value and, consequently, the absorbing surface into a new position from where it captures further material. The rearrangement process drives the previous value of the radius, which we will call $r(t)$ to the value $R(t)$. The simplest manner of describing the process is through

$$\frac{dr(t)}{dt} + \alpha[r(t) - R(t)] = 0 \tag{22}$$

[5] Incidentally, the full approximation means taking the upper limit in the evaluation of $A(t)$ to infinity and that is never a good approximation at small times. But that has little relevance to our present analysis.

where α is the rate of the rearrangement process. In the Laplace domain, this leads to

$$\widetilde{r}(\epsilon) = \frac{r(0)}{\epsilon+\alpha} + \frac{\alpha\widetilde{R}(\epsilon)}{\epsilon+\alpha} \rightarrow \left(\frac{\alpha}{\epsilon+\alpha}\right)\widetilde{R}(\epsilon). \tag{23}$$

The extreme right-hand side expression applies at large times with respect to $1/\alpha$ when the memory of the initial value $r(0)$ is lost and the old and new values of the radius of the disk are seen to be related to each other through a convolution.

This slaving of the variable r by the driving variable R is the origin of the memory arising from the rearrangement process. We have borrowed this concept from its use in the analysis of the nonadiabatic nonlinear dimer performed long ago by Kenkre and Wu [55–57]. In that analysis the driving and driven variables were the vibrational displacement and the site probability difference respectively. Here they are simply the radius of the disk before and after the rearrangement process.

7. Conclusions

While the theory of coalescence we have constructed above is far from a finished task, there being several elements to be worked on as we shall state explicitly below, we believe we have achieved a reasonably satisfactory understanding of the processes involved in the experiments cited. The following discussion should clarify what we have in hand and what needs to be done.

7.1. Essence of the theory proposed in this work

The theory of coalescence we have constructed above is based on simple statistical mechanical considerations of a general nature rather than on specific mechanisms that might be operating in the system considered. We believe we have achieved a reasonably satisfactory understanding of the process involved in the type of experiment cited. A capture process leading to aggregation after rearrangement, the incorporation of the rearrangement in general terms via a time-dependent capture, and the specific representation of the time-dependence by a memory function are the elements of the theory. That coalescence of signal clusters occurs in the experiment [4,5] was quite clear on observation in the laboratory. How it can be described theoretically was the problem that needed to be solved. What was accessible in the literature for this purpose was not sufficient. There were two primary limitations to what was available. There was a general tendency towards using perfect absorber analysis that entails first passage times and the assumption that reaction–diffusion phenomena involve only infinitely fast capture. And where this was supplemented by separate considerations of capture, it was generally assumed that it could be treated by multiplying a probability associated by the capture process to one associated by the motion process.

This probability multiplication prescription cannot be used in reaction–diffusion unless the two processes, motion and capture, are independent of each other. The situation and analysis were similar to those that had occurred decades earlier in the literature on Frenkel exciton motion and capture in molecular crystals and photosynthetic units. Lessons learned in that field [38] were useful to the theory reported here.

7.2. Further comments

Coalescence is a degree more complicated than the simple reaction–diffusion process encountered in trapping or photosynthesis. It has feedback features that had to be respected in our analysis. Explicit comparison to experiment, carried out by us during the process of construction of various stages of our analysis uncovered what was lacking in the analysis. We found that the straightforward application of a reaction–diffusion scheme predicted a growth curve for the radius of the aggregated cluster that was characterized by a single time constant. The experiment clearly predicted a two-time constant curve.

There was no escaping the fact that a significant departure from usual theories of reaction–diffusion was necessary. We argued that the fact that clearly two time-separated processes, one a capture of material and the other a rearrangement in the capturing disk, caused the accumulation process. The time separation idea led us to develop a reaction–diffusion process with *time-dependent* capture. To incorporate such time dependence into the reaction–diffusion formalism was not trivial analytically. A memory function approach to capture, based on the convolution-kind slaving relationship between the disk radius $r(t)$ before the rearrangement process and $R(t)$ after the process,

$$r(t) = \int_0^t ds\phi(t-s)R(s), \tag{24}$$

led to satisfactory fit to observations. Note that the memory $\phi(t)$ naturally occurs as $\alpha e^{-\alpha t}$ so that one returns to an instantaneous relationship as $1/\alpha$, the characteristic time of the rearrangement process memory tends to zero making $\phi(t)$ a δ-function. The approach also allowed us to extract in the process, values for the capture rate constant C and the time for rearrangement $1/\alpha$ both of which appeared to be reasonable for the underlying processes.

Often, particularly in biological systems, memory functions with forms richer than the simple exponential appear as a consequence of the complexity of the underlying processes. For our experiments analyzed in this paper, it has been

unnecessary to introduce this complexity: adequate fitting of data with our theory has been possible with the simple exponential memory. However, it is wise to be on the lookout for a greater degree of richness in the reorganization process underlying the coalescence. We plan to do this in future investigations on other systems where it may be necessary to consider, for instance, power kernel memories. Such power dependences are ubiquitous in biological systems. We have not discussed the relevant formalism here for a reason. The purpose of the present manuscript has been to focus on the problem of time-varying capturing region solved in the manner shown; we have thought it advisable not to dilute the idea by including an analysis of power memories in this same publication.

Among items that remain to be developed are the inclusion of power kernel memories and the study of their consequences, the incorporation of the coalescence of moving particles outside the disk into independent centers, the interactions and coalescence of those finite-size particles with one another, and the relaxation of simplistic considerations that we have used by restricting the analysis to highly symmetrical disk shapes of the forming centers. It is our intention to pursue them in future studies.

Declaration of competing interest

The authors declare that they have no known competing financial interests or personal relationships that could have appeared to influence the work reported in this paper.

Acknowledgments

This work was supported by the National Institute of General Medical Sciences, USA of the National Institutes of Health under award number 1R15GM128166-01 (to K.S.). The content is solely the responsibility of the authors and does not necessarily represent the official views of the National Institute of Biomedical Imaging and Bioengineering, the National Institute of General Medical Sciences, or the National Institutes of Health.

References

[1] I.J. Uings, S.N. Farrow, Cell receptors and cell signalling, J. Clin. Pathol. - Mol. Pathol. 53 (2000) 295–299, http://dx.doi.org/10.1136/mp.53.6.295.
[2] K. Murphy, P. Travers, P. Walter, Janeway's Immunobiology, seventh ed., Garland Science, Taylor and Francis Group, LLC, 2007.
[3] R.M. Weis, K. Balakrishnan, B.A. Smith, H.M. McConnell, Stimulation of fluorescence in a small contact region between rat basophil leukemia cells and planar lipid membrane targets by coherent evanescent radiation, J. Biol. Chem. 257 (1982) 6440–6445, http://dx.doi.org/10.1016/s0021-9258(20)65161-4.
[4] A. Carroll-Portillo, K. Spendier, J. Pfeiffer, G. Griffiths, H. Li, K. Lidke, J. Oliver, D. Lidke, J. Thomas, B. Wilson, J. Timlin, Formation of a mast cell synapse: FcϵRI membrane dynamics upon binding mobile or immobilized ligands on surfaces, J. Immunol. 184 (2010) http://dx.doi.org/10.4049/jimmunol.0903071.
[5] K. Spendier, A. Carroll-Portillo, K.A. Lidke, B.S. Wilson, J.A. Timlin, J.L. Thomas, Distribution and dynamics of rat basophilic leukemia immunoglobulin E receptors (FcϵRI) on planar ligand-presenting surfaces, Biophys. J. 99 (2010) 388–397, http://dx.doi.org/10.1016/j.bpj.2010.04.029.
[6] R. Machado, J. Bendesky, M. Brown, K. Spendier, G.M. Hagen, Imaging membrane curvature inside a FcϵRI-centric synapse in RBL-2H3 cells using TIRF microscopy with polarized excitation, J. Imaging 5 (2019) 63, http://dx.doi.org/10.3390/jimaging5070063.
[7] R. Drawbond, K. Spendier, TIRF microscope image sequences of fluorescent IgE-FcϵRI receptor complexes inside a FcϵRI-centric synapse in RBL-2H3 cells, Data 4 (2019) http://dx.doi.org/10.3390/data4030111.
[8] K. Spendier, J. Thomas, Spatial patterns in mast cell activation, in: Mast Cells: Phenotypic Features, Biological Functions and Role in Immunity, Nova Science Publishers, Inc., 2013.
[9] C.R.F. Monks, B.A. Freiberg, H. Kupfer, N. Sciaky, A. Kupfer, Three-dimensional segregation of supramolecular activation clusters in T cells, Nature 395 (1998) 82–86, http://dx.doi.org/10.1038/25764.
[10] W.S. Hae, P. Tolar, S.K. Pierce, Membrane heterogeneities in the formation of B cell receptor-Lyn kinase microclusters and the immune synapse, J. Cell Biol. 182 (2008) 367–379, http://dx.doi.org/10.1083/jcb.200802007.
[11] S.Y. Qi, J.T. Groves, A.K. Chakraborty, Synaptic pattern formation during cellular recognition, Proc. Natl. Acad. Sci. USA 98 (2001) 6548–6553, http://dx.doi.org/10.1073/pnas.111536798.
[12] T.R. Weikl, R. Lipowsky, Pattern formation during T-cell adhesion, Biophys. J. 87 (2004) 3665–3678, http://dx.doi.org/10.1529/biophysj.104.045609.
[13] M.T. Figge, M. Meyer-Hermann, Modeling receptor-ligand binding kinetics in immunological synapse formation, Eur. Phys. J. D 51 (2009) 153–160, http://dx.doi.org/10.1140/epjd/e2008-00087-1.
[14] P.K. Tsourkas, N. Baumgarth, S.I. Simon, S. Raychaudhuri, Mechanisms of B-cell synapse formation predicted by Monte Carlo simulation, Biophys. J. 92 (2007) 4196–4208, http://dx.doi.org/10.1529/biophysj.106.094995.
[15] P.K. Tsourkas, M.L. Longo, S. Raychaudhuri, Monte Carlo study of single molecule diffusion can elucidate the mechanism of B cell synapse formation, Biophys. J. 95 (2008) 1118–1125, http://dx.doi.org/10.1529/biophysj.107.122564.
[16] P.K. Tsourkas, S. Raychaudhuri, Modeling of B cell synapse formation by monte carlo simulation shows that directed transport of receptor molecules is a potential formation mechanism, Cell. Mol. Bioeng. 3 (2010) 256–268, http://dx.doi.org/10.1007/s12195-010-0123-1.
[17] M. Smoluchowski, Über brownsche molekularbewegung unter einwirkung äußere kräfte und deren zusammenhang mit der verallgemeinerten diffusionsgleichung, Ann. Der Phys. 48 (1915) 1103–1112.
[18] E. Ruckenstein, B. Pulvermacher, Kinetics of crystallite sintering during heat treatment of supported metal catalysts, AIChE J. 19 (1973) 356–364, http://dx.doi.org/10.1002/aic.690190222.
[19] D. Kashchiev, Nucleation: Basic Theory and Applications, Butterworth-Heinemann, 2000, 2000.
[20] V.M. Kenkre, P. Reineker, Exciton Dynamics in Molecular Crystals and Aggregates, in: Springer Tracts in Modern Physics, vol. 94, Springer, Berlin, Heidelberg, 1982.
[21] V.M. Kenkre, Y.M. Wong, Theory of exciton migration experiments with imperfectly absorbing end detectors, Phys. Rev. B 22 (1980) 5716–5722, http://dx.doi.org/10.1103/PhysRevB.22.5716.

[22] V.M. Kenkre, Y.M. Wong, Effect of transport coherence on trapping: Quantum-yield calculations for excitons in molecular crystals, Phys. Rev. B 23 (1981) 3748–3755, http://dx.doi.org/10.1103/PhysRevB.23.3748.
[23] V.M. Kenkre, A theoretical approach to exciton trapping in systems with arbitrary trap concentration, Chem. Phys. Lett. 93 (1982) 260–263, http://dx.doi.org/10.1016/0009-2614(82)80135-8.
[24] V.M. Kenkre, P.E. Parris, Exciton trapping and sensitized luminescence: A generalized theory for all trap concentrations, Phys. Rev. B 27 (1983) 3221–3234, http://dx.doi.org/10.1103/PhysRevB.27.3221.
[25] V.M. Kenkre, D. Schmid, Comments on the exciton annihilation constant and the energy transfer rate in naphthalene and anthracene, Chem. Phys. Lett. 94 (1983) 603–608, http://dx.doi.org/10.1016/0009-2614(83)85066-0.
[26] V.M. Kenkre, P.E. Parris, D. Schmid, Investigation of the appropriateness of sensitized luminescence to determine exciton motion parameters in pure molecular crystals, Phys. Rev. B 32 (1985) 4946–4955, http://dx.doi.org/10.1103/PhysRevB.32.4946.
[27] K. Spendier, V. Kenkre, Analytic solutions for some reaction-diffusion scenarios, J. Phys. Chem. B 117 (2013) http://dx.doi.org/10.1021/jp406322t.
[28] J. Crank, Free and Moving Boundary Problems, Oxford University Press Inc., New York, 1987.
[29] L.T. Adzhemyan, A.N. Vasil'ev, A.P. Grinin, A.K. Kazansky, Self-similar solution to the problem of vapor diffusion toward the droplet nucleated and growing in a vapor-gas medium, Colloid J. 68 (2006) 381–383, http://dx.doi.org/10.1134/S1061933X06030173.
[30] S.I. Barry, J. Caunce, Exact and numerical solutions to a Stefan problem with two moving boundaries, Appl. Math. Model. 32 (2008) 83–98, http://dx.doi.org/10.1016/j.apm.2006.11.004.
[31] H.L. Frisch, F.C. Collins, Diffusional processes in the growth of aerosol particles. II, J. Chem. Phys. 21 (1953) 2158–2165, http://dx.doi.org/10.1063/1.1698803.
[32] F.C. Goodrich, On diffusion-controlled particle growth: The moving boundary problem, J. Phys. Chem. 70 (1966) 3660–3665, http://dx.doi.org/10.1021/j100883a049.
[33] T.A. Witten, L.M. Sander, Diffusion-limited aggregation, a kinetic critical phenomenon, Phys. Rev. Lett. 47 (1981) 1400–1403, http://dx.doi.org/10.1103/PhysRevLett.47.1400.
[34] P. Jensen, A.L. Barabasi, H. Larralde, S. Havlin, H.E. Stanley, Deposition, diffusion, and aggregation of atoms on surfaces: A model for nanostructure growth, Phys. Rev. B 50 (1994) 15316–15329, http://dx.doi.org/10.1103/PhysRevB.50.15316.
[35] J. Abate, W. Whitt, A unified framework for numerically inverting Laplace transforms, INFORMS J. Comput. 18 (2006) 408–421, http://dx.doi.org/10.1287/ijoc.1050.0137.
[36] D.P. Gaver, Observing stochastic processes, and approximate transform inversion, Oper. Res. 14 (1966) 444–459, http://dx.doi.org/10.1287/opre.14.3.444.
[37] A. Fort, V. Ern, V. Kenkre, Theory of coherence effects in time-dependent delayed fluorescence. II. Application to two- and three-dimensional crystals, Chem. Phys. 80 (3) (1983) 205–211, http://dx.doi.org/10.1016/0301-0104(83)85273-2.
[38] V.M. Kenkre, Memory Functions, Projection Operators, and the Defect Technique: Some Tools of the Trade for the Condensed Matter Physicist, Springer Nature, 2021, Chapter 11.
[39] S. Sugaya, V.M. Kenkre, Analysis of transmission of infection in epidemics: Confined random walkers in dimensions higher than one, Bull. Math. Biol. 80 (12) (2018) 3106–3126, http://dx.doi.org/10.1007/S11538-018-0507-2.
[40] V.M. Kenkre, L. Giuggioli, Theory of the Spread of Epidemics and Movement Ecology of Animals: An Interdisciplinary Approach using Methodologies of Physics and Mathematics, Cambridge University Press, 2021, http://dx.doi.org/10.1017/9781108882279.
[41] A. Szabo, G. Lamm, G.H. Weiss, Localized partial traps in diffusion processes and random walks, J. Stat. Phys. 34 (1984) 225–238, http://dx.doi.org/10.1007/BF01770356.
[42] H.S. Carslaw, C.J. Jaeger, Conduction of Heats in Solids, Oxford University Press Inc., New York, 1959.
[43] J.L. Thomas, T.J. Feder, W.W. Webb, Effects of protein concentration on IgE receptor mobility in rat basophilic leukemia cell plasma membranes, Biophys. J. 61 (1992) 1402–1412, http://dx.doi.org/10.1016/S0006-3495(92)81946-X.
[44] J.L. Thomas, D. Holowka, B. Baird, W.W. Webb, Large-scale co-aggregation of fluorescent lipid probes with cell surface proteins., J. Cell Biol. 125 (1994) 795–802.
[45] R.G. Posner, K. Subramanian, B. Goldstein, J. Thomas, T. Feder, D. Holowka, B. Baird, Simultaneous cross-linking by two nontriggering bivalent ligands causes synergistic signaling of IgE FcϵRI complexes, J. Immunol. 155 (1995) 3601–3609.
[46] K. Spendier, TIRF microscopy image sequences of FcϵRI-centric synapse formation in RBL-2H3 cells dataset, Mendeley Data V1 (2020) http://dx.doi.org/10.17632/6KVZV95W7R.1.
[47] D.L. Kolin, P.W. Wiseman, Advances in image correlation spectroscopy: Measuring number densities, aggregation states, and dynamics of fluorescently labeled macromolecules in cells, Cell Biochem. Biophys. 49 (2007) 141–164, http://dx.doi.org/10.1007/s12013-007-9000-5.
[48] C.A. Schneider, W.S. Rasband, K.W. Eliceiri, NIH image to ImageJ: 25 years of image analysis, Nature Methods 9 (2012) 671–675, http://dx.doi.org/10.1038/nmeth.2089.
[49] P. Rogne, M. Rosselin, C. Grundström, C. Hedberg, U.H. Sauer, M. Wolf-Watz, Molecular mechanism of ATP versus GTP selectivity of adenylate kinase, Proc. Natl. Acad. Sci. USA 115 (2018) 3012–3017, http://dx.doi.org/10.1073/pnas.1721508115.
[50] K.A. Henzler-Wildman, M. Lei, V. Thai, S.J. Kerns, M. Karplus, D. Kern, A hierarchy of timescales in protein dynamics is linked to enzyme catalysis, Nature 450 (2007) 913–916, http://dx.doi.org/10.1038/nature06407.
[51] E.W. Montroll, B.J. West, On an enriched collection of stochastic processes, in: Fluctuation Phenomena, North-Holland, Amsterdam, 1979.
[52] V.M. Kenkre, F.J. Sevilla, Thoughts About Anomalous Diffusion: Time-Dependent Coefficients Versus Memory Functions, in: Contributions in Mathematical Physics, Hindustan Book Agency, Gurgaon, 2007, pp. 147–160, http://dx.doi.org/10.1007/978-93-86279-33-0{_}6.
[53] A.A. Ierides, V.M. Kenkre, Reservoir effects on the temperature dependence of the relaxation to equilibrium of three simple quantum systems, Physica A 503 (2018) 9–25, http://dx.doi.org/10.1016/j.physa.2018.02.210.
[54] V.M. Kenkre, A.A. Ierides, Vibrational relaxation of a molecule in strong interaction with a reservoir: Nonmonotonic temperature dependence, Phys. Lett. A 382 (2018) 1460–1464, http://dx.doi.org/10.1016/j.physleta.2018.04.010.
[55] V.M. Kenkre, H.L. Wu, Time evolution of the nonadiabatic nonlinear quantum dimer, Phys. Rev. B 39 (1989) 6907–6913, http://dx.doi.org/10.1103/PhysRevB.39.6907.
[56] V.M. Kenkre, H.L. Wu, Interplay of quantum phases and non-linearity in the non-adiabatic dimer, Phys. Lett. A 135 (1989) 120–124, http://dx.doi.org/10.1016/0375-9601(89)90657-9.
[57] V.M. Kenkre, The quantum nonlinear dimer, in: S. Pnevmatikos, T. Bountis, S. Pnevmatikos (Eds.), Singular behavior and Nonlinear Dynamics, World Scientific, Singapore, 1989, pp. 698–717.